Lumped parameter sensitivity analysis of a distributed hydrological model within tropical and temperate catchments

Lan Cuo,[1]* Thomas W. Giambelluca[2] and Alan D. Ziegler[2,3]

[1] *Institute of Tibetan Plateau Research, Chinese Academy of Sciences, Beijing, 10085, China*
[2] *Department of Geography, University of Hawai'i at Mānoa, Honolulu, 96822, USA*
[3] *Department of Geography, National University of Singapore, Singapore*

Abstract:

Parameter sensitivity of the Distributed Hydrology-Soil-Vegetation Model (DHSVM) was studied in two contrasting environments: (1) Pang Khum Experimental Watershed (PKEW) in tropical northern Thailand; and (2) Cedar River basin (CRB) in Washington State of the temperate US Pacific Northwest. The analysis shows that for both basins, the most sensitive soil parameters were porosity, lateral saturated hydraulic conductivity, and the exponential decrease rate of lateral saturated hydraulic conductivity with soil depth. The most sensitive vegetation parameters were leaf area index, vegetation height, vapour pressure deficit, minimum stomatal resistance (for both grassland and forest scenarios), hemisphere fractional coverage, overstory fractional coverage, and trunk space (for the forest scenario only). Parameter sensitivity was basin-specific, with the humid, temperate CRB being more influenced by vegetation parameters, while tropical PKEW was more influenced by soil properties. Increases and decreases in parameter values resulted in opposite and unequal changes in bias and root mean square error (RMSE), indicating the non-linearity of physical process represented in the hydrological model. Copyright © 2011 John Wiley & Sons, Ltd.

KEY WORDS   distributed hydrological model; lumped parameter sensitivity

Received 28 March 2009; Accepted 20 January 2011

INTRODUCTION

Optimisation of physics-based land-surface models would not be necessary if (1) parameters, site-specific constants, and forcing data could be prescribed accurately from measurements; and (2) the models themselves represented governing physical laws related to energy and mass exchange in land and atmosphere adequately (Bastidas *et al*., 2006). However, in practice, these criteria are difficult to achieve and parameter estimation procedures are necessary. The complexity of models and the large number of parameters make optimisation difficult. Sensitivity analysis speeds the calibration and validation process by identifying which parameters produce the largest changes in model output in response to perturbations (Demaria *et al*., 2007; Scollo *et al*., 2008). By isolating the most influential parameters, sensitivity analysis can guide research prioritisation in both observation and modelling fields (Prihodko *et al*., 2008). Sensitivity analysis also provides insight into the treatment of particular processes (e.g. evapotranspiration and runoff generation) in land surface models and hence can be used to diagnose the behaviour of land surface models (Wilson *et al*., 1987a,b; Abramopolous

et al., 1988; Mahfouf and Jacquemin, 1989; Henderson-Sellers, 1992; Pitman, 1994; Gao *et al*., 1996; Liang and Guo, 2003; Demaria *et al*., 2007; van Werkhoven *et al*., 2008a).

Saltelli (1999), Bastidas *et al*. (2006), and Tang *et al*. (2007) provided detailed descriptions of sensitivity analysis approaches that have been commonly used in land surface modelling. Each of the many approaches available has its strengths and weaknesses (Gao *et al*., 1996). In general, two kinds of sensitivity analysis have been widely used: local and global methods. In the local approach, parameter values are varied within specified ranges relative to baseline values, which are usually the means of the parameter ranges. One-factor-at-a-time (e.g. Wilson *et al*., 1987a,b; Pitman 1994; Gao *et al*., 1996), differential analysis (e.g. Doherty, 2003; Tang *et al*., 2007; Bahremand and Smedt, 2007), and fractional factorial analysis (Henderson-Sellers, 1992; Liang and Guo, 2003) are examples of local sensitivity analysis approaches. On the other hand, the global approach, such as regional sensitivity analysis (Spear and Hornberger, 1980; Spear *et al*., 1994; Franks and Beven, 1997; Demaria *et al*., 2007) and variance-based sensitivity analysis (Tang *et al*., 2007; Scollo *et al*., 2008; van Werkhoven *et al*., 2008a), examines parameters in their entire physical ranges. Global sensitivity analysis uses various sampling methods (e.g. random sampling, systematic random sampling) to test parameter values

* Correspondence to: Lan Cuo, Institute of Tibetan Plateau Research, Chinese Academy of Sciences, Beijing, 10085, China.
E-mail: cuol@u.washington.edu

distributed across their respective ranges. Hence, it can provide a complete picture of parameter interaction and corresponding model response. Consequently, the number of model runs required for global sensitivity analysis is large (Satelli *et al.*, 2008; Demaria *et al.*, 2007). In contrast, the local approach has the features of simplicity and low computation demand, but cannot account for effects of parameter interaction (Gao *et al.*, 1996).

One-factor-at-a-time (OFAT) has often been used to diagnose land surface models and has proven to be a useful approach (e.g. Wilson *et al.*, 1987a,b; Pitman 1994; Gao *et al.*, 1996; Sun and Bosilovich, 1996). In this study, we used the OFAT method to study parameter sensitivity for a distributed hydrology model. While previous applications of the OFAT approach employed a single statistical objective function and a more or less arbitrary perturbation range, we used two objective functions, bias and RMSE, and, in most cases, used the standard deviation to set the perturbation range (in some cases, the lower limit of the parameter range was used). Using the OFAT approach, we examined parameter sensitivity of the Distributed Hydrology-Soil-Vegetation Model (DHSVM version 2·0) for both a tropical monsoon catchment in northern Thailand and a catchment in the cool, humid US Pacific Northwest. The main objective of this study is to identify individual parameters that are important for the simulation of energy, soil moisture, and streamflow variables in two contrasting environments. The study will guide both future field observation priorities and aid future DHSVM calibration and validation.

STUDY AREAS

Pang Khum experimental watershed

The 94-ha Pang Khum Experimental Watershed (PKEW) was established in 1997 near the village of Pang Khum (19°03′N, 98°39′E), Chiang Mai Province, Thailand (Figure 1). PKEW is part of the Mae Taeng River basin, which is a headwater catchment of the Ping River that eventually flows into the Chao Phraya River. PKEW lies in a mountainous region alternately affected by the southwesterly Indian summer monsoon and the northeasterly Asian winter monsoon. The study area has distinct wet and dry seasons which is typical of southeast Asia monsoon climate: approximately 90% of the annual precipitation occurs between May and November. Snowfall is insignificant. Baseflow gradually declines beginning in December from its relatively high wet-season level, with the lowest flows typically occurring just prior to the onset of the wet season in April or May. Based on 10 years of measurements (1996–2005), annual precipitation is 1800 mm, and mean annual temperature minima and maxima are 8 and 34 °C, respectively. The original tropical evergreen (with pine) forest has been altered by timber removal and swidden cultivation, including, prior to the early 1990s, intensive opium cultivation (Ziegler *et al.*, 2004). Around 18% of the area in PKEW was used actively or inactively as agricultural land based on a 2002 field survey. Soils are predominantly Ultisols; and the major soil texture is sandy clay loam (Ziegler, 2000). The underlying geology is largely granite with some gneiss present. Elevation ranges from approximately 1100 to 1600 m (Figure 1). Slopes range from
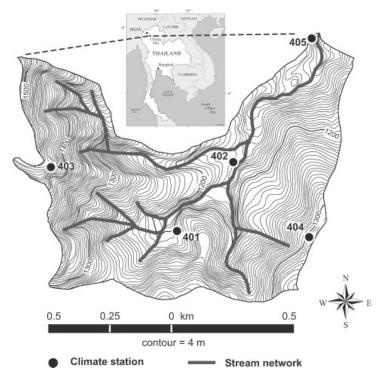

Figure 1. Topography and location of hydro-climate stations in Pang Khum Experimental Watershed (PKEW) in tropical northern Thailand. 401 and 402 are climate and soil moisture stations; 403 and 404 are soil moisture stations; 405 is a stream gauge
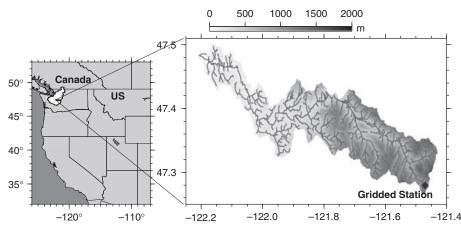
Figure 2. Geographical location and elevation map of Cedar River basin

0 to 48° (based on a 5-m DEM). Soils are generally deeper in this area compared to the US Pacific Northwest. PKEW has two climate stations (Figure 1): one within an advanced secondary forest (401); the other in a swidden field (402). Two additional stations measure soil moisture (403 and 404); a fifth station records stream discharge at the basin outlet (405). Meteorological data, recorded at 20-min intervals from August 1997 to December 2000, were aggregated to hourly for this analysis. Measured forcing data included air temperature (°C), wind speed (m s^{-1}), relative humidity (%), incoming shortwave radiation (W m^{-2}), near-surface soil temperature (°C), and rainfall (m). Downward longwave radiation (W m^{-2}) was calculated as the residual in the radiation balance equation based on measured net radiation, downward and reflected short wave radiation, and outgoing longwave radiation. Soil temperature was estimated from mean annual air temperature during the study period (20 °C).

Cedar River basin

The Cedar River basin (CRB), which drains to Puget Sound, is located on the west slope of the Cascade Mountain range in Washington State (Figure 2). The climate is maritime temperate, and precipitation is strongly winter-dominant, occurring mostly between November and April. Much of the basin lies in the transient snow zone, where the form of precipitation changes from rain to snow many times each winter. The CRB is the source of the City of Seattle's drinking water supply. The area of the CRB is about 469 km^2, and elevation ranges from sea level to 1600 m. Based on 88 years (1915–2002) of climate data, annual precipitation in CRB is about 2100 mm. Low flow conditions predominate from May to October. Mean annual minimum and maximum temperatures are 2·6 and 12·6 °C, respectively. Soils are mainly sandy loam, loamy sand, and loam; and the most extensive soil class is sandy loam. Vegetation is primarily coniferous forest in the upland and mixed coniferous and deciduous in the lowland. Logging in this region started in the late 19th century when European settlement began, and this continues up to the present. Early timber harvesting was primarily in the lowlands, and now has moved to the uplands. Much of the basin has been preserved since the 1950s. Based on a 2002 land cover map (Alberti *et al*., 2004), about 10% of the land in Cedar River basin has been harvested.

Station data interpolated to a grid (gridded stations) were used to drive the Cedar basin model. The gridding procedure followed Maurer *et al*., (2002) and Hamlet and Lettenmaier (2005) and is described by Cuo *et al*., (2009). Daily interval station data used in the gridding process
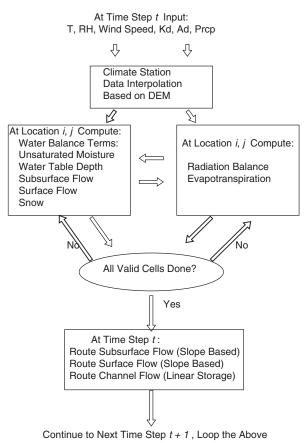

Figure 3. DHSVM 2·0 structure and flow chart

Table I. Means, standard deviations (SD), ranges, and sources of soil and vegetation parameters used for sensitivity test in PKEW and CRB

Parameters	Abbrev.	Description	mean ±SD/quantitative range[a]	mean ±SD/quantitative range[b]	Sources
Soil parameters					
Lateral saturated hydraulic conductivity (ms^{-1})	K_{ls}	Used in calculation of lateral flow movement	3.24e6 ± 5.98e6	1.17e5 ± 1.37e5	Meyer et al., 1997
Exponential decrease rate of K_{ls} with soil depth	EDR	Exponent describing the decrease of K_{ls} with soil depth	0.03 ± 0.2	0.03 ± 0.2	Calculated from Giambelluca, 1996; Ziegler, 2000
Maximum infiltration capacity (ms^{-1})	MIC	Maximum rate of soil infiltration	3.24e6 ± 5.98e6	1.17e5 ± 1.37e5	Meyer et al., 1997
Porosity (m^{3}m^{-3})	P	Soil moisture content at saturation	0.53 ± 0.07	0.346 ± 0.0915	Giambelluca, 1996[a]; Ziegler, 2000[a]; Meyer et al., 1997[b]
Pore size distribution index	PSD	Used in Brooks-Corey equation	0.479 ± 0.127	0.892 ± 0.155	Meyer et al., 1997
Bubbling pressure (m)	h_b	Used in the soil desorption to the air	0.262 ± 0.213	0.177 ± 0.120	Meyer et al., 1997
Field capacity (m^{3}m^{-3})	f_c	Used to estimated available water for subsurface layers	0.212 ± 0.0568	0.116 ± 0.0369	Meyer et al., 1997
Wilting point (m^{3}m^{-3})	w_p	Used in the evapotranspiration calculation	0.12 ± 0.0214	0.0659 ± 0.0179	Meyer et al., 1997
Bulk density (kgm^{-3})	BD	Used to estimate dry soil thermal conductivity	1198 ± 229	1198 ± 229	Giambelluca, 1996; Ziegler, 2000
Vertical saturated hydraulic conductivity (ms^{-1})	K_{vs}	Determines vertical water movement	3.24e6 ± 5.98e6	1.17e5 ± 1.37e5	Meyer et al., 1997
Soil thermal conductivity (Wm^{-1}K^{-1})	STC	Used in calculation of soil heat flux	0–2.68	0–2.68	Rosenberg et al., 1983
Soil volumetric thermal capacity (Jm^{-3}K^{-1})	SVTC	Used in calculation of soil surface energy balance	0.3e6–6.0e6	0.3e6–6.0e6	Rosenberg et al., 1983
Soil surface albedo	SSALB	The same as above	0.05–0.45	0.05–0.45	Rosenberg et al., 1983
Vegetation parameters					
Overstory vegetation height (m)[c]	OVH	Used in calculation of aerodynamic resistance	5–120	5–120	Field observation
Understory vegetation height (m)	UVH	The same as above	0.3–3.3	0.3–3.3	Breuer et al., 2003
Canopy overstory fractional coverage[c]	OFC	Used in calculation of evapotranspiration	0–1	0–1	Field observation
Hemisphere fractional coverage[c]	HFC	Used in calculation of radiation balance	0–1	0–1	Field observation
Trunk space (fraction)[c]	TS	Used in calculation of aerodynamic resistance	0–1	0–1	Field observation
Maximum stomatal resistance (sm^{-1})	R_{smax}	Used in calculation of canopy resistance	0–4.7e5	0–4.7e5	http://research.esd.ornl.gov/~hnw/ARMCarbon/SiB/sibrc.pdf
Minimum stomatal resistance (sm^{-1})	R_{smin}	Used in calculation of canopy resistance	0–250	0–250	Rosenzweig and Abramopoulos, 1997

Parameter	Abbreviation	Description			Source
Soil moisture threshold for transpiration (m³ m⁻³)	MT	Used in calculation of canopy resistance	0.12 ± 0.021	0.0659 ± 0.0179	Meyer et al., 1997
Overstory leaf area index[c]	OLAI	Used in calculation of canopy resistance, snow interception, radiation balance	$2.55-7.99$	6.3 ± 4.3	Herbert and Fownes, 1997[a]; de Wasseige et al., 2003[a]; Breuer et al. 2003[b]
Understory leaf area index	ULAI	The same as above	2.92 ± 1.15	6.2 ± 3.8	Giambelluca, 1996[a]; Ziegler, 2000[a]; Breuer et al. 2003[b]
Overstory albedo[c]	OALB	Used in calculation of radiation balance	0.16 ± 0.022	0.125 ± 0.04	Giambelluca, 1996[a]; Ziegler, 2000[a]; Breuer et al. 2003[b]
Understory albedo	UALB	The same as above	0.167 ± 0.018	0.23 ± 0.07	Giambelluca, 1996[a]; Ziegler, 2000[a]; Breuer et al. 2003[b]
Aerodynamic extinction factor[c]	AEF	Used in calculation of aerodynamic resistance	$1.88-3.54$	$1.88-3.54$	Goudriaan, 1977
Clumping factor[c]	CF	Used in calculation of radiation balance	$0.6-1$	$0.6-1$	Chen et al., 1997
overstory vapour pressure deficit above which transpiration is restricted (Pa)[c]	OVPD	Used in calculation of canopy resistance	2090 ± 845	2090 ± 845	Giambelluca, 1996; Ziegler, 2000
Understory vapour pressure deficit (Pa)	UVPD	The same as above	2045 ± 861	2045 ± 861	Giambelluca, 1996; Ziegler, 2000
Scattering parameter[c]	SP	Used in calculation of radiation balance	$0.7-0.85$	$0.7-0.85$	Nijssen and Lettenmaier, 1999
Rpc (fraction)	—	Used in calculation of canopy resistance	$0.001-0.95$	$0.001-0.95$	Sellers et al., 1994
Maximum snow interception capacity (fraction)[c]	MSIC	Used in calculation of canopy snow interception	0.055 ± 0.06	0.055 ± 0.06	Breuer et al., 2003 and Model default
Snow interception efficiency[c]	SIE	The same as above	$0-1$	$0-1$	Model default
Mass release drip ratio[c]	MRDR	Used in calculation of snow interception and snow fall on the ground	$0-1$	$0-1$	Model default
Root zone depth (m)	RZD	Used in calculation of available moisture, evapotranspiration,	2.1 ± 1.31	2.1 ± 1.31	Breuer et al., 2003
Overstory root zone fraction[c]	ORZF	The same as above	$0-1$	$0-1$	Model default
Understory root zone fraction	URZF	The same as above	$0-1$	$0-1$	Model default

[a] Parameter settings for PKEW.
[b] Parameter settings for CRB.
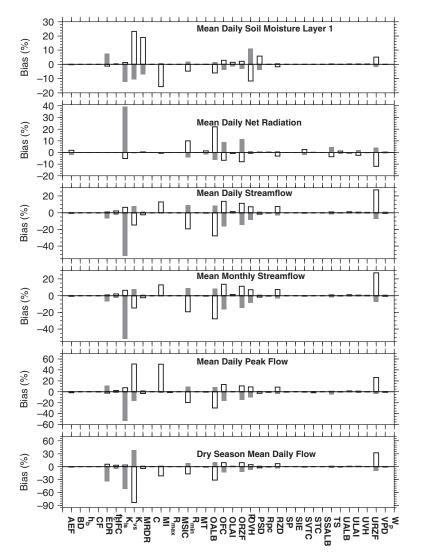[c] Overstory parameter (not used in grassland scenario).

Figure 4. Bias due to increase and decrease of parameter values for the forest scenario in PKEW. Lateral and vertical hydraulic conductivity, exponential decrease rate of lateral hydraulic conductivity, and maximum infiltration capacity were increased by one standard deviation and decreased to the lower limits of their respective ranges. Other parameters were changed by plus and minus one standard deviation. Gray bars (empty bars) indicate the result of a parameter increase (decrease). The same notion for the following bias figures. Parameter notion is the same as in Table I

were from National Climate Data Center (NCDC). Daily data were interpolated to a 3-h time step to provide a reasonable representation of the diurnal cycles in solar radiation and surface air temperature. Soil temperature of 5 °C was estimated from mean annual air temperature during the study period and was used for calculating soil-sensible heat flux and energy balance.

MODEL

Model description

DHSVM, version 2·0, incorporates physical processes including canopy interception, evapotranspiration, energy and radiation balance, saturation-excess overland flow, infiltration-excess overland flow, ground water recharge, snow accumulation and melt, unsaturated soil moisture movement, and saturated subsurface flow (Figure 3 for DHSVM flow chart, and

http://www.hydro.washington.edu/Lettenmaier/Models/DHSVM/overview.shtml for DHSVM schematics). Catchment spatial characteristics are explicitly accounted for using grids (geo-referenced raster datasets) to represent the spatial distributions of elevation, soil properties, vegetation properties, stream, and/or road networks. A Digital Elevation Model (DEM) is used to direct downslope water movement and to extrapolate climate data. Soil and vegetation properties are represented by grid cells in correspondence with the boundary and resolution of the DEM. Each grid cell has user-specified root-zone fractions, root-zone depths, and vegetation layers. Overstory coverage (specified as canopy closure) in each cell is variable; understory, if present, covers the entire cell. Saturated subsurface flow is largely controlled by the lateral hydraulic conductivity. Unsaturated soil moisture movement in the root zones and deep soil layer above the water table is controlled by the vertical saturated
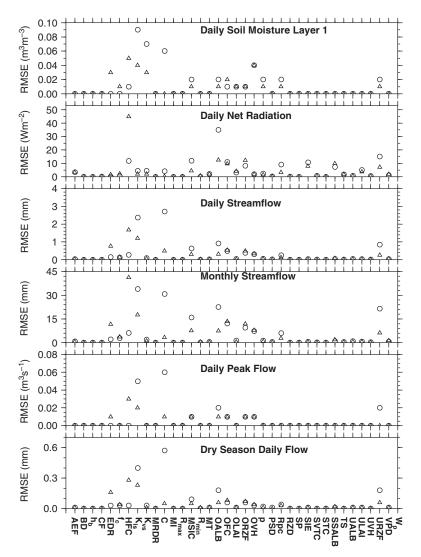
Figure 5. Root mean square error (RMSE) due to parameter change for the forest scenario in PKEW. Triangles (circles) represent results of parameter value increase (decrease). Symbols are the same for the following RMSE figures

hydraulic conductivity which can be different for different soil layers. DHSVM parameters can be classified into soil, vegetation (or land cover), elevation, stream, road, and radiation categories. DHSVM has been applied in both tropical (Cuo *et al*., 2006, 2008; Thanapakpawin *et al*., 2007) and temperate catchments (e.g. Pacific NW in North America: Storck *et al*., 1998; Bowling *et al*., 2000; La Marche and Lettenmaier, 2001; VanShaar *et al*., 2002; Thyer *et al*., 2004; Cuo *et al*., 2009). However, these studies did not analyse parameter sensitivity specifically and only showed calibration and validation results. Detailed descriptions of DHSVM can be found in Wigmosta *et al*., (1994 and 2002).

Model implementation

In PKEW, a 50-m DEM was extracted from a 1 : 4000 scale 4-m-interval topographic contour map generated from aerial photos. A 150-m DEM was used in the larger CRB study catchment. Soil textures in the model were sandy clay loam and sandy loam for PKEW and CRB, respectively. The time step was one hour for the PKEW simulations and three hours for the CRB simulations. Stream network and morphology were generated from Arcinfo macro language scripts (DHSVM website, http://www.hydro.washington.edu/Lettenmaier/Models/DHSVM/index.shtml, accessed 1 August 2009). Known constants, such as temperature lapse rate, precipitation lapse rate, ground roughness, snow roughness, rain/snow partition thresholds, snow water capacity, and LAI multipliers for rain and snow interception were set to model defaults (DHSVM website). Sky view and hourly sun shading parameters related to watershed terrain were generated using programs provided on the DHSVM website; these were considered as constants and not changed in the sensitivity analysis. Although DHSVM has an algorithm that represents the effects of forest roads on runoff (e.g. Storck *et al*., 1998; Cuo *et al*., 2006), it was not implemented in this study.
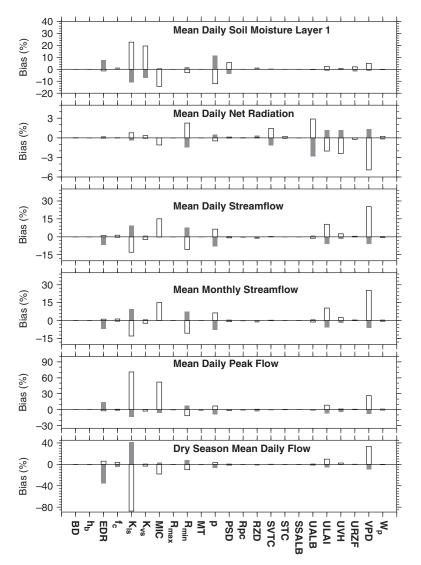
Figure 6. Bias for the grassland scenario in PKEW

In the original model setup, there were multiple soil and vegetation types. For example, in PKEW, there were 9 soil classes and 6 vegetation/land cover classes; in CRB, 6 soil classes and 14 vegetation classes. To reduce the number of parameters in the analysis, we used a lumped analysis approach, i.e. we focused on the dominant soil and land cover types in each basin, in this case, forest, and for contrast, grassland cover. These two scenarios represent the end members of all possible land-cover/land-use configurations. All model output variables evaluated in this study were aggregated spatially (basin-wide) and temporally (daily interval). Although all grid cells share the same land cover and soil parameter values in a given model run, the simulation process is still distributed, i.e. the simulation is conducted for each grid cell, lateral surface and subsurface flows are represented, and streamflow is routed at each time step.

For the forest scenario, 13 soil and 23 vegetation parameters were investigated, and for the grassland scenario, 13 soil and 10 vegetation parameters (Table I). The

lower number of vegetation parameters in the grassland scenario reflects the absence of overstory canopy parameters. Some of the soil and vegetation parameters in PKEW were based on field measurements. Most parameters for CRB were derived from published values for similar environments. When no literature values or measurements were available, model defaults or approximations were used. Values for maximum infiltration capacity and lateral saturated hydraulic conductivity (K_{ls}) were assumed to be the same as vertical saturated hydraulic conductivity (K_{vs}). The moisture threshold below which transpiration ceases was assumed to be the same as the wilting point. In CRB, soil depth of 2–3 m was assumed and used in the model. In PKEW, average soil depths of 6–7 m were used. Soil depth is greater in valleys and shallower on ridges. In both basins, the model was initialized using forcing for the period 1 August 1997–31 December 1998, and parameter-sensitivity analysis was performed for the period 1 January 1999–31 December 2000.
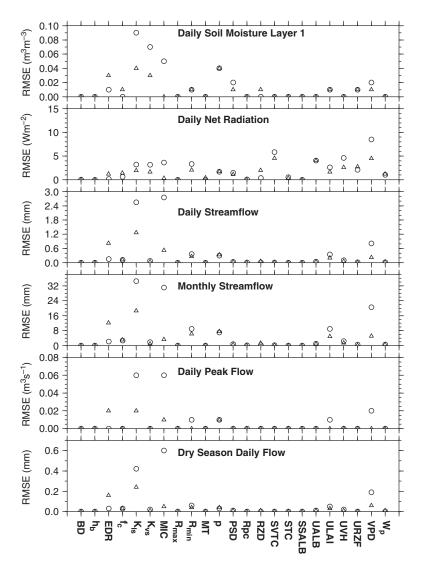
Figure 7. RMSE for the grassland scenario in PKEW

PARAMETER SENSITIVITY ANALYSIS

The OFAT method has been used to diagnose land surface models. Wilson *et al*. (1987a) used OFAT to examine the Biosphere Atmosphere Transfer Scheme (BATS) representation of soil characteristics. OFAT was also used to test the sensitivity of BATS simulations to parameter values by Pitman (1994) and Gao *et al*., (1996) and to investigate the land surface parameterisation of the NCAR Community Climate Model (Wilson *et al*., 1987b). Similar studies were done by Abramopolous *et al*., (1988) and Mahfouf and Jacquemin (1989). These previous studies showed that OFAT is a valuable approach. Unlike previous studies, the objective of this paper is to identify sensitive parameters but not to diagnose the hydrology model. Given the simplicity of OFAT approach, testing the sensitivity of a single model output variable and using a single objective function could result in misleading information. In this study, we examined multiple variables simulated by the model representing energy balance, soil moisture,

and streamflow response. Parameter sensitivity was tested using two objective functions (bias and RMSE).

Sensitivity analysis focused on the effects of parameter perturbations of plus and minus one standard deviation on simulated basin aggregated daily net radiation (W m^{-2}), first-layer daily wet season soil moisture (m^3 m^{-3}), daily and monthly streamflow (mm), daily peak flow (m^3 s^{-1}), and dry season daily flow (mm). Daily peak flow was calculated by first averaging the flows in each day, then identifying the flows that were higher than those of the preceding and succeeding days. For parameters for which only the range was known, the mean and standard deviations were calculated assuming a uniform distribution:

$$\text{Mean}: \quad \frac{a+b}{2} \qquad (1)$$

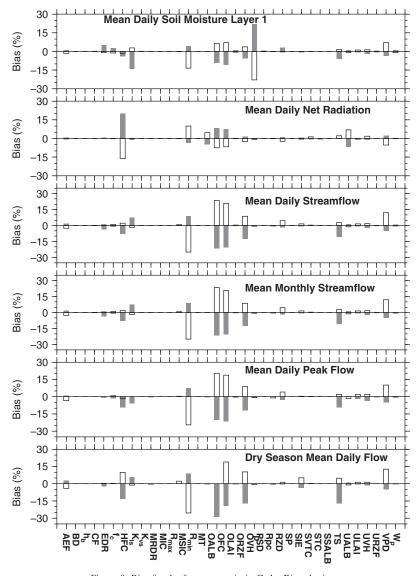$$\text{Standard deviation}: \quad \sqrt{\frac{(b-a)^2}{12}} \qquad (2)$$

Figure 8. Bias for the forest scenario in Cedar River basin

where *a* and *b* are the lower and upper boundaries of the range.

DHSVM was first run using mean values of all soil and vegetation parameters to derive reference time series of daily net radiation, daily wet season soil moisture, daily streamflow, monthly streamflow, daily peak flow, and daily dry season flow. For the experimental runs (36 runs for forest and 23 runs for grassland), all parameter values were increased and decreased by one standard deviation, while keeping the others at their specified mean values, except when a decrease of one standard deviation resulted in a negative value. Exponential decrease rate of saturated hydraulic conductivity, saturated lateral and vertical hydraulic conductivity, and maximum infiltration capacity were decreased to the lower limit of their range. Results from experimental runs were compared with those from the control run rather than with a parameter-optimized run from Cuo *et al*., (2006 and 2009), which were not available for both catchments.

Although optimized parameters had been obtained for one of the basins (PKEW, Cuo *et al*., 2006, 2009), we chose to conduct the sensitivity testing in the pre-optimized mode. This approach corresponds to the usual case for those conducting sensitivity analysis, i.e. sensitivity testing is usually done prior to model optimisation. This approach also recognizes that optimized parameter values are conditional, being dependent on model structure, other parameter values used in the simulation, the calibration period, and the objective functions considered (Mahfouf and Jacquemin, 1989; Franks and Beven, 1997; Yapo *et al*., 1998; van Werkhoven, 2008b).

Bias and RMSE were calculated from the control and experimental runs at daily and monthly (for streamflow only) time steps. To calculate bias, the study-period averages of the simulated time series of daily streamflow, net radiation, and wet season soil moisture were used.
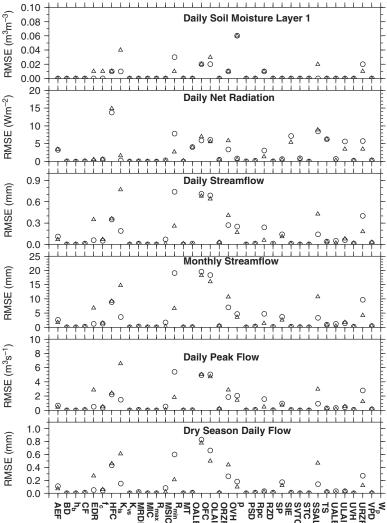
Figure 9. RMSE for the forest scenario in Cedar River basin

RESULTS

Parameter sensitivity summary

Bias and RMSE values resulting from positive and negative parameter perturbations for forest and grassland simulations are shown in Figures 4–11. Perturbation of vapour pressure deficit, minimum stomatal resistance, and leaf area index resulted in large changes in soil moisture, net radiation, and discharge in both the tropical PKEW and temperate CRB catchments. The differences between forest and grassland are mostly a result of obvious differences in vegetation structure represented in the model. Overstory parameters are not used in the grassland scenario, and understory parameters are important for grassland than for forest (Figures 4–11). Sensitivity of some parameters is basin-specific. For example, soil moisture and average flow are sensitive to vertical saturated hydraulic conductivity and maximum infiltration capacity in PKEW (Figures 4–7), but not in CRB (Figures 8–11). In some cases, parameters were found to be sensitive based on either bias or RMSE,

but not both. Also, positive and negative parameter perturbations resulted in opposite but unequal changes in output variables (Figures 4–11).

Table II summarizes the top five (in case of a tie, there are more than five) sensitive parameters, based on both bias and RMSE, for the forest and grassland scenarios. In general, the following parameters were deemed the most sensitive because perturbations caused large changes in output variables, net radiation (Rnet), soil moisture (SM), and streamflow (Q, including all aspects of a hydrograph examined), irrespective of the basin.

PKEW and CRB Forest

- Lateral saturated hydraulic conductivity (SM, Q)
- Exponential decrease rate of K_{ls} (Q)
- Porosity (SM)
- Minimum stomatal resistance (Q, Rnet, SM)
- Overstory vegetation height (Q)
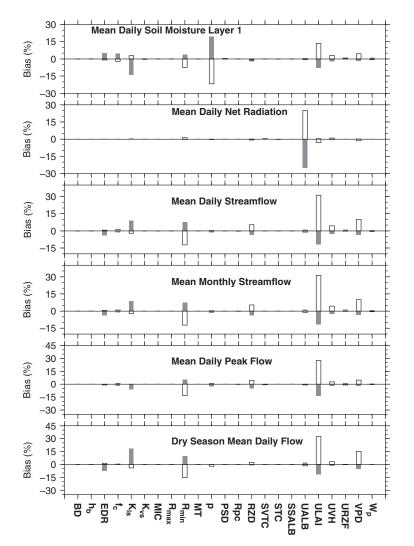- Overstory LAI (Rnet, Q, SM)

Figure 10. Bias for the grassland scenario in Cedar River basin

- Canopy overstory fractional coverage (Rnet, Q)
- Hemisphere fractional coverage (Rnet, Q)
- Trunk space (Rnet, Q)
- Overstory vapour pressure deficit (Rnet, SM, Q)

PKEW and CRB grassland

- Lateral saturated hydraulic conductivity (SM, Q)
- Exponential decrease rate of K_{ls} (Q)
- Porosity (SM)
- Minimum stomatal resistance (Q, Rnet, SM)
- Understory LAI (Q)
- Understory albedo (Rnet)
- Understory vapour pressure deficit (Q, Rnet, SM)
- Understory vegetation height (Rnet, Q)
- Root zone depth (Rnet, Q)

Six vegetation and four soil parameters were insensitive: i.e. perturbations caused minimal modelled output changes in either basin:

- Bulk density

- Bubbling pressure
- Clumping factor
- Moisture threshold
- Soil surface albedo
- Maximum stomatal resistance
- Rpc
- Maximum snow interception capacity
- Mass release drip ratio
- Scattering parameter

Soil surface albedo was not sensitive because our specification of forest and grassland vegetation classes dictated that the soil surface was completely covered by vegetation.

The most important vegetation parameters for forest are hemisphere fractional coverage, overstory LAI, overstory vegetation height, minimum stomatal resistance, overstory vapour pressure deficit, overstory fractional coverage and trunk space. Most of these parameters are associated with the overstory vegetation structure and used in the calculation of wind and radiation attenuation
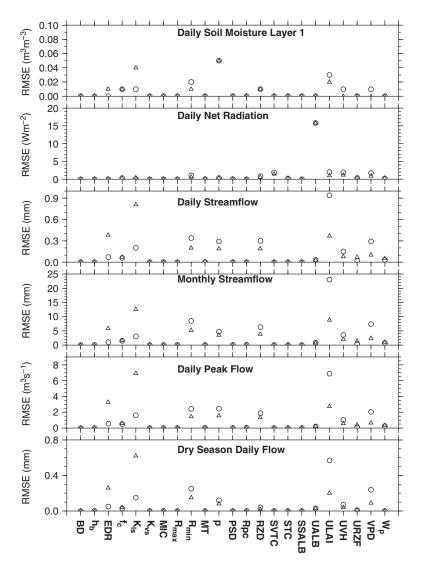
Figure 11. RMSE for the grassland scenario in Cedar River basin

through the overstory canopy (Nijssen and Lettenmaier, 1999). In addition to their roles in intercepting radiation and affecting the wind profile, overstory fractional coverage and LAI also determine the amount of precipitation intercepted by the canopy. Thus, these parameters strongly influence the partitioning of water among evapotranspiration, soil moisture storage, and streamflow components. For grassland, understory albedo, understory LAI, understory vapour pressure deficit, and understory vegetation height and parameters associated with the soil surface are the most important in controlling the partitioning of simulated energy and water variables.

The most important soil parameters are porosity, lateral saturated hydraulic conductivity, and the change of hydraulic conductivity with soil depth. Porosity determines the maximum soil water content. Lateral saturated hydraulic conductivity controls the rate of water movement in the soil column. Porosity and lateral saturated hydraulic conductivity, together, to a large extent,

determine the partition of water between the soil column and stream channel. Maximum infiltration capacity did not affect streamflow in PKEW when it was shifted downward, perhaps implying that the mean value obtained from the literature and measurement is too high.

Basin sensitivity

Table II shows that, in the forest scenario, soil moisture is more sensitive to soil parameters in PKEW than in CRB. Flow variables, including mean daily (monthly) flow, peak flow, and dry season flow, are more sensitive to vegetation parameter control than soil moisture in both basins. In PKEW, soil parameters exert more control on flow than in CRB. Net radiation is controlled mostly by vegetation parameters in both basins. In CRB, soil volumetric thermal capacity also has some influence on net radiation.

For the grassland scenario (Table II), soil moisture was influenced by more soil parameters in PKEW than in CRB. Vegetation properties are more important in CRB

Table II. Most (top 5, in case of a tie, there are more than 5) sensitive parameters based on bias and RMSE calculations for forest and grassland scenarios in PKEW and CRB

	CRB		PKEW	
	Vegetation	Soil	Vegetation	Soil
Forest simulation (+ one standard deviation)				
First layer daily soil moisture	OLAI, OFC, TS	K_{ls}, p SVTC	HFC	EDR, K_{ls}, K_{vs}, p
Daily net radiation	HFC, OALB, OFC, OLAI, OVH, TS, UALB	K_{ls},	HFC, OFC, OVH, OLAI, TS	EDR, K_{ls}, MIC
Daily/monthly streamflow	OFC, OLAI, OVH, Rsmin, TS	K_{ls}	HFC, OFC, OLAI, OVH, Rsmin	EDR, K_{ls}, p
Daily peak flow	HFC, OFC, OLAI, OVH, TS	K_{ls}	HFC, OFC, OLAI, OVH, Rsmin	EDR, K_{ls}
Dry season daily streamflow	HFC, OFC, OLAI, OVH, TS		HFC, OFC, OLAI, OVH, OVPD	
Forest simulation (− one standard deviation)				
First layer daily soil moisture	OFC, OLAI, OVPD, Rsmin	P SVTC	OFC, OVPD, Rsmin, RZD	K_{ls}, K_{vs}, MIC, p, PSD
Daily net radiation	HFC, OFC, OLAI, Rsmin, TS, UALB,	SVTC	OFC, OVH, OLAI, OVPD, Rsmin	
Daily/monthly streamflow	HFC, Rsmin, OFC, OLAI, OVH, OVPD		OFC, OLAI, OVPD, Rsmin	K_{ls}, MIC
Daily peak flow	HFC, Rsmin, OFC, OLAI, OVH, OVPD		OFC, OVH, OLAI, OVPD, Rsmin	K_{ls}, MIC, p
Dry season daily streamflow	HFC, Rsmin, OLAI, OVH, OVPD		OFC, OVPD, Rsmin	K_{ls}, MIC
Grassland simulation (+ one standard deviation)				
First layer daily soil moisture	Rsmin, RZD, ULAI,	EDR, f_c, K_{ls}, p SVTC	Rsmin, RZD, ULAI, URZF, UVPD	EDR, f_c, K_{ls}, K_{vs}, p, PSD SVTC
Daily net radiation	Rsmin, RZD, UALB, ULAI, UVH		Rsmin, UALB, UVH, URZF, UVPD	
Daily/monthly streamflow	Rsmin, RZD, ULAI	EDR, K_{ls}, p	Rsmin, UVPD	EDR, K_{ls}, MIC, p
Daily peak flow	Rsmin, RZD, ULAI	EDR, K_{ls}, p	Rsmin, UVPD	EDR, K_{ls}, MIC, p
Dry season daily streamflow	Rsmin, ULAI, UVPD	EDR, K_{ls}	Rsmin, UVPD	EDR, K_{ls}, MIC, p
Grassland simulation (− one standard deviation)				
First layer daily soil moisture	Rsmin, RZD, ULAI, UVH, UVPD	f_c, K_{ls}, p SVTC	UVPD	K_{ls}, K_{vs}, MIC, p, PSD SVTC
Daily net radiation	Rsmin, UALB, ULAI, UVH, UVPD	P	Rsmin, UALB, ULAI, UVH, UVPD	
Daily/monthly streamflow	Rsmin, RZD, ULAI, UVH, UVPD	P	Rsmin, ULAI, UVPD	K_{ls}, MIC
Daily peak flow	Rsmin, RZD, ULAI, UVH, UVPD	P	Rsmin, ULAI, UVPD	K_{ls}, MIC, p
Dry season daily streamflow	Rsmin, ULAI, UVH, UVPD	K_{ls}, p	Rsmin, ULAI, UVPD	K_{ls}, MIC

Parameters are listed in alphabetical order; abbreviations are shown in Table I.

Table III. Comparison of parameter sensitivity as identified by bias and root mean square error (RMSE). S: both bias and RMSE found the same parameters to be sensitive; D: bias and RMSE identified different sensitive parameters. The analysis was not restricted to the top 5 sensitive parameters as shown in Table II, and thus not directly comparable to Table II

Basins	CRB				PKEW			
Land cover scenario	Forest		Grassland		Forest		Grassland	
Parameter change	Increased	Decreased	Increased	Decreased	Increased	Decreased	Increased	Decreased
First layer daily soil moisture	S	D	S	S	S	D	S	S
Daily net radiation	D	D	D	D	S	D	D	S
Daily/monthly streamflow	D	D	D	D	D	S	D	S
Daily peak flow	D	D	D	D	D	D	D	S
Dry seasonal daily flow	S	D	D	S	D	S	S	S

than in PKEW in the flow simulation. Soil properties do not strongly control net radiation. Soil parameters are more important in the flow and soil moisture simulation for the grassland than for the forest.

Bias vs RMSE

Sensitive parameters are generally identifiable in terms of both bias and RMSE. However, in some cases, bias and RMSE analyses identified different parameters as being most sensitive. Table III shows similarities and differences in results obtained by bias and RMSE analyses for six variables in CRB and PKEW, for both forest and grassland. For first-layer soil moisture, sensitivity based on bias and RMSE give similar results. For peak flow, however, bias and RMSE analyses mostly give different results. When decreasing parameter values in PKEW grassland, bias and RMSE analyses resulted in equivalent sensitivity rankings.

Non-linearity

Figures 4–11 show comparisons of parameter value increases and decreases in PKEW and CRB for forest and grassland. In general, perturbations of sensitive parameters produce large bias and RMSE values regardless of whether the parameter values are increased or decreased. However, in some cases, an increase (decrease) caused large change, but decrease (increase) caused minimal to small change, for example, hemisphere fractional coverage, vapour pressure deficit, and maximum infiltration capacity in the PKEW forest scenario, and minimum stomatal resistance in the CRB forest scenario. Although an increase in a parameter value always results in bias in the opposite direction of that resulting from a decrease in the parameter, the figures show that the size of the biases in opposite directions generally differ, reflecting the non-linear model response.

DISCUSSION

OFAT analysis is largely consistent with experience gained in the prior model calibration in PKEW and CRB (Cuo *et al*., 2006, 2009) and confirms the importance of soil hydraulic properties such as lateral saturated hydraulic conductivity and porosity for simulating

streamflow and soil moisture variables. The study also identified the importance of forest canopy characteristics indicating that using the default forest canopy parameter values may not improve calibration in some basins.

Wagener *et al*., (2009) found that parameter sensitivity for streamflow simulation depends on which statistical objective function is used. The current study confirms that parameter sensitivity depends on the choice of statistical objective function for soil moisture, net radiation and streamflow variables (Figures 4–11). Thus, it is necessary to examine both bias and RMSE to identify sensitive parameters. Depending on the variables examined, the difference could be minimal or large.

Van Werkhoven *et al*., (2008a) analysed the Sacramento Soil Moisture Accounting Model simulated streamflow using multiple objective functions that represent various aspects of the hydrograph, and found that parameter sensitivities varied with the averaging period. Here, we analysed mean daily and monthly streamflow in PKEW and CRB. Obviously, bias was not affected by the averaging period. For the RMSE analysis (Figures 4, 5, 6, and 7), the same parameters were found to be sensitive, but to different extents. The difference in parameter sensitivity implies that good daily streamflow calibration does not necessarily assure good monthly streamflow simulation, and vice versa.

The two study basins were distinct in climate, soil, and vegetation. The analysis showed that parameter sensitivity was basin-specific, which is in agreement with previous studies (Bastidas *et al*., 2006; van Werkhoven *et al*., 2008a). The main differences between PKEW and CRB parameter sensitivity are in vegetation and soil property dominance. In Cedar, overstory properties have more weight than in PKEW for simulating soil moisture and streamflow. Soil properties are more important in PKEW than in CRB.

The major differences in the model setup between two basins were the basin size (PKEW: 1 km^2, CRB: 469 km^2), grid cell resolution (PKEW: 50 m; CRB: 150 m) and model running time step (PKEW:1 h; CRB: 3 h). In this study, we used spatially and temporarily aggregated variables to minimize the effects of the differences in model setup. If the simulation results were analysed in distributed mode and the time step

were not aggregated to daily, but remained model-dependent, the setup differences could have more effect on the sensitivity results. For example, Liang *et al*., (2004) found that Variable Infiltration Capacity-model parameters calibrated at a coarse resolution can be applied to finer resolutions to obtain generally comparable results, however, the reverse is not reliably applicable.

One limitation of this study is the uncertainty in the estimated means and standard deviations of some parameters in Table I. The statistics of some parameters may not accurately represent those of their populations because of limited sample sizes. For example, the statistics of overstory albedo for temperate coniferous forest were derived from 19 samples (Breuer *et al*., 2003), while about 106 samples of coniferous LAI were used to infer its mean and standard deviation (Breuer *et al*., 2003). The uncertainty in parameter statistics could help to explain, to some extent, the lack of sensitivity of vertical saturated hydraulic conductivity and maximum infiltration capacity in CRB, and of overstory albedo and the positive shift in maximum infiltration capacity in PKEW. The limitation may also help to explain the non-linear response of the model to increases and decreases in parameter values. These parameter sampling issues call for more field measurement of overstory albedo, vertical saturated hydraulic conductivity, and maximum infiltration capacity in the respective environments.

Parameter sensitivity analysed in a basin-averaged format at an averaged daily time step (with uniform land cover and soil types) is able to identify basin-wide and basin-specific parameter sensitivity which satisfies the goal of the study. However, the analysis cannot account for the spatial variability of parameter sensitivity in individual basins. It was previously shown that DHSVM parameter sensitivity (for streamflow) is spatially variable in PKEW (Cuo, 2005). For example, within PKEW, the sensitive soil and vegetation parameters of cells located close to the basin outlet had more influence on streamflow than parameter values in other cells. Van Werkhoven *et al*., (2008b) also found that model parameter sensitivity varies with rainfall distribution and the location of the cell in relation to the basin outlet. To study the spatial variability of parameter sensitivity in individual basins, distributed analysis should be followed.

CONCLUSION

Using one-factor-at-a-time analysis, this study compared parameter sensitivity in simulating energy balance and hydrological variables in a tropical and a temperate catchment. Bias and RMSE of net radiation, soil moisture, daily and monthly average flow, peak flow, and dry season flow were examined by increasing and decreasing DHSVM parameter values for forest and grassland scenarios. Parameter sensitivity was found to be both basin-specific and statistical objective function-specific. The increase and decrease of parameter values caused bias in opposite directions, but usually in unequal amounts,

demonstrating the non-linear model response to some variables. The lack of sensitivity of the model to overstory albedo in PKEW, and vertical saturated hydraulic conductivity and maximum infiltration capacity in CRB, may have resulted from insufficient parameter sample sizes, suggesting the need for more field observation.

Regardless of basin (tropical *versus* temperate) or land cover scenario (forest *versus* grassland), the following parameters should be given special attention during model calibration: lateral saturated hydraulic conductivity, exponential decrease rate of K_{ls}, porosity, minimum stomatal resistance, vegetation height, LAI, and vapour pressure deficit. For forested catchments, canopy overstory fractional coverage, hemisphere fractional coverage and trunk space are also important. More attention should be given to vegetation parameters in catchments located in humid marine temperate climates than in tropical monsoon climates. Also, calibration efforts should place more emphasis on the soil and understory properties when grassland is a dominant land cover.

REFERENCES

Abramopolous F, Rosenzweig C, Choudhury B. 1988. Improved ground hydrology calculation for global climate models (GCMs): soil water movement and evapotranspiration. *Journal of Climate* **1**: 921–941.

Alberti M, Weeks R, Coe S. 2004. Urban land cover change analysis in central Puget Sound. *Photogrammetric Engineering & Remote Sensing* **70**: 1043–1052.

Bahremand A, De Smedt F. 2007. Distributed hydrological modeling and sensitivity analysis in Torysa Watershed, Slovakia. *Water Resource Manage* **22**: 393–408.

Bastidas LA, Hogue TS, Sorooshian S, Gupta HV. 2006. Parameter sensitivity analysis for different complexity land surface models using multicriteria methods. *Journal of Geophysical Research* **111**: D20101, DOI:10.1029/2005JD006377.

Bowling L, Storck P, Lettenmaier DP. 2000. Hydrologic effects of logging in western Washington, United States. *Water Resources Research* **36**(11): 3223–3240.

Breuer L, Echhardt K, Frede H-G. 2003. Plant parameter values for models in temperate climates. *Ecological modeling* **169**: 237–293.

Chen JM, Blanken PD, Black TA, Guilbeault M, Chen S. 1997. Radiation regime and canopy architecture in a boreal aspen forest. *Agricultural and Forest Meteorology* **86**: 107–125.

Cuo L. 2005. Effects of land cover and rural roads on hydrological processes in mountainous watersheds in Northern Thailand. Ph.D. dissertation. University of Hawaii at Manoa, Hawaii, USA.

Cuo L, Giambelluca TW, Ziegler AD, Nullet M. 2006. Use of the distributed hydrology soil vegetation model to study road effects on hydrological processes in Pang Khum Experimental Watershed, Northern Thailand. *Forest Ecology and Management* **224**: 81–94.

Cuo L, Giambelluca TW, Ziegler AD, Nullet MA. 2008. The roles of roads and agricultural land use in altering hydrological processes in

Nam Mae Rim watershed, northern Thailand. *Hydrological Processes* **22**: 4339–4354.

Cuo L, Lettenamaier DP, Alberti M, Richey JE. 2009. Effects of a century of land cover and climate change on the hydrology of the Puget Sound basin. *Hydrological Processes* **23**: 907–933.

Demaria EM, Nijssen B, Wagener T. 2007. Monte Carlo sensitivity analysis of land surface parameters using the Variable Infiltration Capacity model. *Journal of Geophyiscal Research* **112**: D11113, DOI:10.1029/2006JD007534.

de Wasseige C, Bastin D, Defourny P. 2003. Seasonal variation of tropical forest LAI based on field measurements in Central African Republic. *Agricultural and Forest Meteorology* **119**: 181–194.

Doherty J. 2003. Ground water model calibration using pilot points and regularization. *Ground Water* **41**(2): 170–177.

Franks SW, Beven KJ. 1997. Bayesian estimation of uncertainty in land surface-atmosphere flux predictions. *Journal of Geophysical Research* **102**(D20): 23991–23999.

Gao X, Sorooshian S, Gupta HV. 1996. Sensitivity analysis of the biosphere-atmosphere transfer scheme. *Journal of Geophysical Research* **101**(D3): 7279–7289.

Giambelluca TW. 1996. Tropical land cover change: Charactering the post forest land surface. In *Climate change: Developing southern hemisphere perspectives*, Giambelluca TW, Henderson-Sellers A (eds). John Wiley and Sons: UK; 293–318.

Goudriaan J. 1977. *Crop micrometeorology: a simulation study*. Centre for Agricultural Publishing and Documentation: Wageningen, The Netherlands.

Hamlet AF, Lettenmaier DP. 2005. Production of temporally consistent gridded precipitation and temperature fields for the continental US. *Journal of Hydrometeorology* **6**(3): 330–336.

Henderson-Sellers A. 1992. Assessing the sensitivity of a land-surface scheme to parameters used in tropical-deforestation experiments. *Quarterly Journal of the Royal Meteorological Society* **118**: 1101–1116.

Herbert DA, Fownes JH. 1997. Effects of leaf aggregation in a broad-leaf canopy on estimates of leaf area index by the gap-fraction method. *Forest Ecology and Management* **97**: 277–282.

La Marche JL, Lettenmaier DP. 2001. Effects of forest roads on flood flows in the Deschutes River, Washington. *Earth Surface Processes and Landforms* **26**: 115–134.

Liang X, Guo J. 2003. Intercomparison of land-surface parameterization schemes: sensitivity of surface energy and water fluxes to model parameters. *Journal of Hydrology* **279**: 182–209.

Liang X, Guo J, Leung LR. 2004. Assessment of the effects of spatial resolutions on daily water flux simulations. *Journal of Hydrology* **298**: 28–310.

Mahfouf J-F, Jacquemin B. 1989. A study of rainfall interception using a land surface parameterization for mesoscale meteorological models. *Journal of Applied Meteorology* **28**: 1280–1302.

Maurer EP, Wood AW, Adam JC, Lettenmaier DP, Nijssen B. 2002. A long-term hydrologically-based data set of land surface fluxes and states for the conterminous United States. *Journal of Climate* **15**: 3237–3251.

Meyer PD, Rockhold ML, Gee GW. 1997. Uncertainty analyses of infiltration and subsurface flow and transport for SDMP sites, NUREG/CR-6565, Pacific Northwest National Laboratory, Richland, Washington.

Nijssen B, Lettenmaier DP. 1999. A simplified approach for predicting shortwave radiation transfer through boreal forest canopies. *Journal of Geophysical Research* **104**(D22): 27859–27868.

Pitman AJ. 1994. Assessing the sensitivity of a land-surface scheme to the parameter values using a single column method. *Journal of Climate* **7**(12): 1856–1869.

Prihodko L, Denning AS, Hanan NP, Baker I, Davis K. 2008. Sensitivity, uncertainty and time dependence of parameters in a complex land surface model. *Agricultural and Forest Meteorology* **148**: 268–287.

Rosenzweig C, Abramopoulos F. 1997. Land-surface model development for the GISS GCM. *Journal of Climate* **10**: 2040–2054.

Saltelli A. 1999. Sensitivity analysis: Could better methods be used? *Journal of Geophysical Research* **104**(D3): 3789–3793.

Saltelli A, Ratto M, Andrei T, Campolongo F, Carboni J, Gabelli D, Saisana M, Tarantola S. 2008. *Global sensitivity analysis. The Primer,* John Wiley & Sons: England.

Scollo S, Tarantola S, Bonadonna C, Coltelli M, Saltelli A. 2008. Sensitivity analysis and uncertainty estimation for tephra disperal model. *Journal of Geophysical Research* **113**: B06202, DOI:10.1029/2006JB004864.

Sellers PJ, Los SO, Tucker CJ, Justice CO, Dazlich DA, Collatz GJ, Randall DA. 1994. A global 1 by 1 degree NDVI data set for climate studies. Part 2: The generation of global fields of terrestrial biophysical parameters from the NDVI. *International Journal of Remote Sensing* **15**(17): 3519–3545.

Spear RC, Hornberger GM. 1980. Eutrophication in peel inlet—II. Identification of critical uncertainties via generalized sensitivity analysis. *Water Research* **14**: 43–49.

Spear RC, Grieb TM, Shang N. 1994. Parameter uncertainty and interaction in complex environmental models. *Water Resources Research* **30**(11): 3159–3169.

Storck P, Bowling L, Wetherbee P, Lettenmaier DP. 1998. Application of a GIS-based distributed hydrology model for prediction of forest harvest effects on peak stream flow in the Pacific Northwest. *Hydrological Processes* **12**: 889–904.

Sun W-Y, Bosilovich MG. 1996. Planetary boundary layer and surface layer sensitivity to land surface parameters. *Boundary-Layer Meteorology* **77**: 353–378.

Tang Y, Reed P, Wagener T, van Werkhoven K. 2007. Comparing sensitivity analysis methods to advance lumped watershed model identification and evaluation. *Hydrology and Earth System Sciences* **11**: 793–817.

Thanapakpawin P, Richey J, Thomas D, Rodda S, Campbell B, Logsdon M. 2007. Effects of landuse change on the hydrologic regime of the Mae Chaem river basin, NW Thailand. *Journal of Hydrology* **334**(1): 215–230.

Thyer M, Beckers J, Spittlehouse D, Alila Y, Winkler R. 2004. Diagnosing a distributed hydrologic model for two high-elevation forested catchments based on detailed stand- and basin-scale data. *Water Resources Research* **40**: W01103, DOI:10.1029/2003WR002414.

van Werkhoven K, Wagener T, Reed P, Tang Y. 2008a. Characterization of watershed model behavior across a hydroclimatic gradient. *Water Resources Research* **44**: W01429, DOI:10.1029/2007WR006271.

van Werkhoven K, Wagener T, Reed P, Tang Y. 2008b. Rainfall characteristics define the value of streamflow observations for distributed watershed model identification. *Geophysical Research Letter* **35**: L11403, DOI:10.1029/2008GL034162.

VanShaar JR, Haddeland I, Lettenmaier DP. 2002. Effects of land-cover changes on the hydrological response of interior Columbia River basin forested catchments. *Hydrological Processes* **16**: 2499–2520.

Wagener T, van Werkhoven K, Reed P, Tang Y. 2009. Multiobjective sensitivity analysis to understand the information content in streamflow observations for distributed watershed modeling. *Water Resources Research* **45**: W02501, DOI:10.1029/2008WR007347.

Wigmosta MS, Vail LW, Lettenmaier DP. 1994. A distributed hydrology-vegetation model for complex terrain. *Water Resources Research* **30**(6): 1665–1679.

Wigmosta MS, Nijssen B, Storck P. 2002. The distributed hydrology soil vegetation model. In *Mathematical models of small watershed hydrology and applications*, Singh VP, Frevert DK (eds). Water Resource Publications: Littleton, CO; 7–42.

Wilson MF, Henderson-Sellers A, Dickinson RE, Kennedy PJ. 1987a. Sensitivity of the Biosphere-Atmosphere Transfere Scheme (BATS) to the inclusion of variable soil characteristics. *Journal of Applied Meteorology and Climatology* **26**: 341–362.

Wilson MF, Henderson-Sellers A, Dickinson RE, Kennedy PJ. 1987b. Investigation of the sensitivity of the land-surface parameterization of the NCAR Community Climate Model in regions of tundra vegetation. *Climatology* **7**: 319–343.

Yapo PO, Gupta HV, Sorooshian S. 1998. Multi-objective global optimization for hydrologic models. *Journal of Hydrology* **204**: 83–97.

Ziegler AD. 2000. Toward modeling erosion on unpaved roads in mountainous Northern Thailand, Ph.D. dissertation, University of Hawaii at Manoa, Hawaii, USA.

Ziegler AD, Giambelluca TW, Sutherland RA, Nullet MA, Yarnasarn S, Pinthong J, Preechapanya P, Jaiaree S. 2004. Toward understanding the cumulative impacts of roads in upland agricultural watersheds of northern Thailand. *Agriculture Ecosystems and Environment* **104**: 145–158.

http://research.esd.ornl.gov/~hnw/ARMCarbon/SiB/sibrc.pdf, accessed on 15 August 2005.